JOURNAL OF AIRCRAFT
Vol. 30, No. 2, March–April 1993

Experimental and Nonlinear Vortex Lattice Method Results for Various Wing-Canard Configurations

J. Rom,* B. Melamed,† and D. Almosnino‡
Technion—Israel Institute of Technology, Haifa 32000, Israel

Experimental measurements of the aerodynamic characteristics of five close-coupled wing-canard configurations up to moderately high angles of attack are used to evaluate the ability of the nonlinear vortex lattice method (NLVLM) to calculate the aerodynamic characteristics of such configurations. The longitudinal aerodynamic coefficients, the rolled-up vortex trajectories, and the pressure distributions are compared for the five wing-canard configurations, as well as for the three wing planforms for which experimental data is available. The investigation includes the effects of varying the canard deflections and the canard positions relative to the wing of the various configurations. The lift- and induced-drag coefficients which are evaluated by the NLVLM for the wing-canard configurations are found to be in good agreement with the experimental data up to the angle of attack of 20–25 deg. The NLVLM works even better for wings alone in that the pitching moment can also be well-predicted. Therefore, this analysis tool can potentially be used in the "design by analysis" process employed during the preliminary design for wing-canard configurations.

Nomenclature

AR = aspect ratio
b = wing span, mm
C_D = induced-drag coefficient based on wing planform area
C_L = lift coefficient based on wing planform area
C_m = pitching moment coefficient based on wing area and wing root chord
C_p = pressure coefficient when Δp is the "lifting" pressure, $\Delta p/0.5\rho_\infty V_\infty^2$
c = wing root chord, mm
D = drag force, kg
H = height of canard above wing plane/c
L = lift force, kg
Re = Reynolds number based on wing root chord
V = velocity, m/s
X = distance from wing apex to canard apex/c
y = coordinate in the spanwise direction/c
α = angle of attack
δ_c = canard deflection angle relative to wing
ρ = density

Subscripts
c = canard
∞ = free stream conditions

Introduction

IT is by now well-established that higher lift coefficients can be achieved on slender wing configurations by the use of aerodynamic means that stabilize the free rolled-up vortices and/or delay vortex breakdown at high angles of attack. At increasing angles of attack, the lift due to these vortices is increasing as long as the rolled-up vortices remain coherent and stable. Such enhancement of the leading-edge vortices is obtained by the close-coupled wing-canard configuration. The canard vortices interact with the wing vortices in such a way as to stabilize the free rolled-up vortices to higher angles of attack and also delay the vortex bursting. This results in the extension of the useful range of the angles of attack enabling higher values for the maximum lift coefficients for the wing-canard configurations. Similar effects of enhancing the coherence of the free rolled-up vortices and delaying vortex breakdown is also achieved by various devices such as leading-edge extensions (LEX), "saw tooth" extensions, strakes and vortex generators, and by blowing of jets.

The close-coupled wing-canard configuration has the additional advantage of utilizing the movable canard as an aerodynamic control surface. In this case the movable canard generates (in addition to its lift and pitching moment) strong vortices that augment the strength of the wing's rolled-up vortices, resulting in an increase of the total lift at higher angles of attack. The flowfield generated at these vortices will cause an upwash on the canard due to the wing, and a downwash on the wing due to the canard that will affect the lift forces and the pitching moments on each one of these surfaces and, therefore, the total lift and the trim and control effectiveness of the wing-canard configuration. In the present investigation we will examine the capabilities of the nonlinear vortex lattice method (NLVLM) to evaluate the aerodynamic characteristics of the wing-canard configuration which is dominated by the interactions between the canard and the wing vortices.

It is generally assumed that the vortex flow over the slender wing with or without the canard can be predicted with relatively good accuracy by inviscid methods of analysis. It is clear that the generation process of the free vortices, which is started by the separation of the vortical shear layer from the body and/or the wing's surface (or at the sharp leading edges), is due to viscous effects. These viscous effects may be viewed as the result of the strong interaction between the viscous flow near the surfaces with the inviscid external flow. It is then assumed that once the shear layers separate from the surfaces or leave the sharp leading edges they then roll up into the known "rolled up vortices," and from then on the resulting flow is dominated by the inviscid vortical flow characteristics. This hypothesis is the justification for the various panel methods as well as the justification for the application of the recently developed Euler code methods (Refs. 1–4). The complexity, the difficulty, and the high costs of the Euler code calculations for practical aerodynamic configurations at subsonic speeds is still rather formidable.[5] One of the objectives

Presented as Paper ICAS 90-334 at the ICAS/AIAA 17th Congress of the International Council of the Aeronautical Sciences, Stockholm, Sweden, Sept. 9–14, 1990; received Dec. 2, 1991; revision received Feb. 21, 1992; accepted for publication Feb. 21, 1992.

*Professor, Lady Davis Chair, Department of Aerospace Engineering. Fellow AIAA.
†Graduate Student, Department of Aerospace Engineering.
‡Research Fellow, Department of Aerospace Engineering.

of this article is to show that it is possible to obtain reasonably accurate values for the aerodynamic characteristics of wing-canard configurations in subsonic flows by the use of the much simpler and the much more economical (in computer resources) NLVLM presented in Refs. 6–9, and an improved version[10] will be used in this article.

The NLVLM is a modification of the classical vortex lattice method (VLM)[11] by adding the effects of the rolling-up of the free vortices in the computation scheme (as detailed in Refs. 6 and 7) for the calculations of the aerodynamic parameters of wings, including the close coupled wing-canard configurations. The application of the NLVLM to slender bodies and lifting surfaces of various cross sections is presented in Refs. 8 and 9. An improved version of the NLVLM is presented in Ref. 10. A brief review of the method and description of the recent improvements in the calculation scheme are included in this article.

Method of Calculation

The first step in the NLVLM calculation is to divide the surfaces of the configuration to small panels (quadrilateral or triangular) and to imbed the appropriate potential singularities in each one of these panels, these are the elementary solutions to the Laplace equation such as horseshoe line vortices and source distributions. In the classical VLM the trailing vortices are kept in the plane of the lifting surfaces, therefore, all the aerodynamic coefficients vary linearly with angle of attack. In the NLVLM the trailing vortices are allowed to detach from the lifting surfaces into the freestream and follow the streamlines into the rolled-up vortex structure. For thick wings and for bodies, the thickness effects are accounted for by the superposition of potential sources which are distributed on the panel surfaces. In the cases of wings with rounded leading edges and bodies of various shapes, it is required to determine (independently) the shape and the position of the separation lines.

The strength of the vortices in each panel and the induced flowfield are then calculated by solving the matrix equation using the procedures presented in Ref. 10. The trailing vortices are allowed to leave the lifting surfaces at all edges and on bodies along specific separation lines. The trajectories of the free vortices are calculated imposing a cutoff distance parameter to join vortices as they approach this limiting distance. The induced velocities and the vortex strengths are calculated by a double iterative procedure—an inner iteration, and then the full iterative cycle. The program was modified to insure better criterion for convergence. The convergence is insured by checking the deviations of the values of the strength of all bound vortices in all panels (as was already done in Ref. 12 for slender bodies) and also the convergence of the trajectories of all free vortices at every point of the calculated trajectories. The application of these two convergence criterions insures that both the lift coefficient and the pitching moment coefficient as well as the pressure distribution are converged.

Close-Coupled Canard-Wing Configurations

Experimental data on five wing-canard configurations (Figs. 1a–e) are available and published in Refs. 13–20. These experiments also include data for the wings along (canard off cases). It is therefore possible to compare the aerodynamic characteristics evaluated by the NLVLM with the experimental data.

Two of these configurations are the European test models used for computer code verification—models A and B, shown in Figs. 1a and 1b. Details of model A are given in Refs. 14 and 15, and the details of model B in Ref. 16. The other three models are the Technion models—the cropped wing-canard, the wide canard, and the narrow canard shown in Figs. 1c, 1d, and 1e, respectively. Details of the cropped wing-canard are given in Ref. 13, and those for the wide and narrow canards in Refs. 17–19.

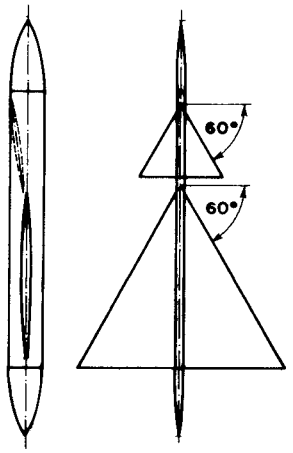

a) European model A

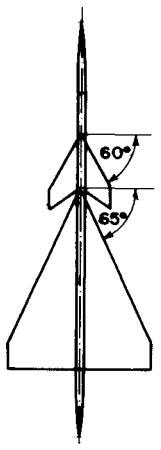

b) European model B

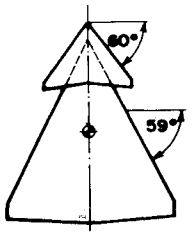

c) Cropped-delta

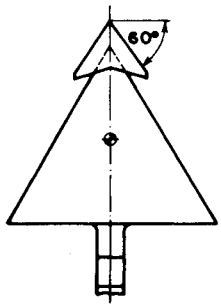

d) Wide canard

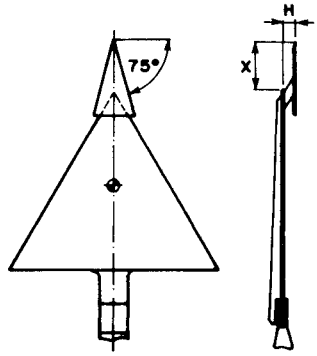

e) Narrow canard

Fig. 1 Five wing-canard models.

The European model A (Fig. 1a) has a 60-deg triangular wing and a 60-deg triangular canard; both wing and canard are of AR = 2.31. The wing span is 600 mm and the canard span is 40% of the wing span. Both are attached to a flat fuselage where the canard can be placed at various vertical and horizontal positions in relation to the wing, and the canard can also be deflected as shown in Fig. 1a. The experiments are conducted with the canard trailing edge just forward of the wing apex, and the canard vertical position is 4% of wing chord above the wing plane.

The European model B (Fig. 1b) has a cropped delta wing with AR = 1.38, 65-deg swept leading edge and the wing span is 412 mm. The canard has 60-deg sweep for the leading edge and 35-deg swept back trailing edge (as seen in Fig. 1b) with AR = 1.65, and the canard span is 44% of the wing span. The horizontal position of the canard is so that the apex of the trailing edge of the canard is at the wing apex and the canard vertical position is at 4% wing chord above the wing plane.

The Technion cropped delta (CD) model (Fig. 1c) is the model investigated in Ref. 13. The wing planform is a moderate AR cropped delta having a triangular angle of 59 deg and AR = 1.85 and a small trailing edge sweep angle of 4.1 deg and the wing span is 212.8 mm. The canard planform is the same as that used in the wide canard model, with AR = 2.9, and an area which is 18% of the wing area and the canard span is 113 mm. The canard can be positioned at various horizontal and vertical stations in relation to the wing. The experiments are conducted for the canard at 9% of wing root chord above the wing plane.

The Technion wide canard (WC) model (Fig. 1d) has a 60-deg triangular wing (AR = 2.31) and the span is 288 mm, and it has a canard which is a cropped delta with a 60-deg swept leading edge and 35-deg swept back trailing edge (AR = 2.9). The Technion narrow canard (NC) model (Fig. 1e) has a 60-deg triangular wing (AR = 2.31) and the span is 288 mm and it has a canard which is a 75-deg swept leading-edge delta (AR = 1). These models are similar to those used in the investigation presented in Ref. 17 except that in the present tests the wing has sharp leading edges and a flat upper surface. The canard can be placed at various vertical and horizontal positions and also can be deflected by the use of a series of spacers. The experiments are conducted for the canard at 14% of wing root chord above the wing plane.

Presentation and Discussion of Results

The NLVLM program enables the calculation of the vortex trajectories, the bound vortex strength (aerodynamic loads) in each panel of the wing and each panel of the canard, as well as the velocity vector field over the configuration and its wake. The results can be presented as aerodynamic forces and moments variation with angle of attack, trajectories of the free vortices over the configuration, and its wake and velocity vector field at various cross sections around the configuration.

As a first test, selected experimental aerodynamic coefficients for the two wing planforms alone (the wings of European models A and B) are compared with the calculated NLVLM results in Figs. 2 and 3. The agreement between the experimental data and the NLVLM calculations is very good for both the lift- and induced-drag coefficients (corrected for the friction drag by subtracting the measured drag at zero angle of attack) as well as for the pitching moment coefficients up to angles of attack of 17–20 deg for the delta wing of model A and up to 25 deg for the cropped delta wing of model B. The NLVLM results are higher than the experimental data for the higher angles of attack since vortex breakdown reaches the trailing edges of these wings at an angle of attack of about 14–17 deg, resulting in a loss of vortex lift and the corresponding effect on the pitching moment. Some of the differences may be attributed to the presence of the fuselage whose effect is to lower the experimental values of the lift coefficients. Comparison of the experimental and calculated lift coefficients of the wing alone of the cropped delta model is included in Fig. 4 where the lift coefficients for the cropped delta canard configuration are also included.

The lift, induced drag, and pitching moment coefficients for the other wing-canard configurations are presented in Figs. 5–8. The results for the European model A at canard deflections of δ_c of -12, 0, and $+12$ deg are presented in Fig. 5, and for model B with zero canard deflection, $\delta_c = 0$, are presented in Fig. 6. Comparing the experimental data and the NLVLM calculated results indicate very good agreement for the lift- and induced-drag coefficients for angles-of-attack of 20 deg and the NLVLM results are only 5% higher at α = 25 deg. However, the pitching moment results are different. There is some agreement at low angles of attack, but large differences at increasing angles of attack.

The effects of canard deflections on the aerodynamic coefficients of the European model A are shown in Fig. 5. The

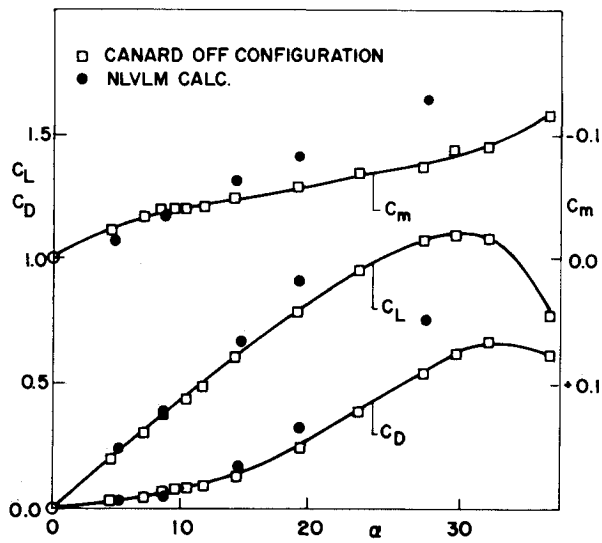

Fig. 2 Aerodynamic coefficients of the 60-deg delta wing.

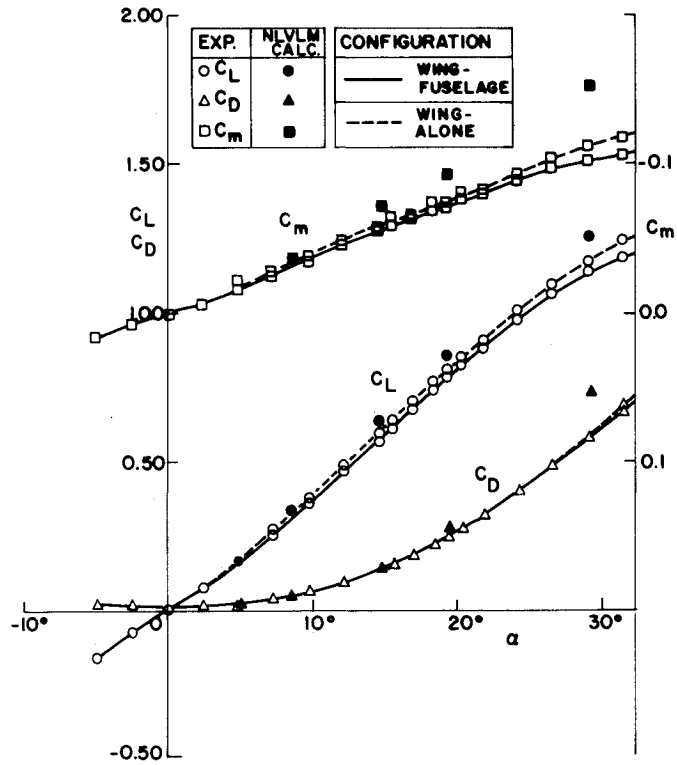

Fig. 3 Aerodynamic coefficients of the wing of model B.

canard deflection has a small effect on the lift coefficient as is well-predicted by the NLVLM calculation. Again, the agreement in the case of the lift coefficient is very good up to 25 deg. In the case of the pitching moment coefficient the NLVLM is able to predict the effect of canard deflection at low angle of attack, but the error becomes large as the angle of attack increases.

The results for the wide canard and narrow canard models are shown in Figs. 7 and 8. The canards are positioned at only one height of 14% wing root chord above the wing since previous investigation (Ref. 13) indicated that the vertical height of the canard when it is above the wing has only a small effect on the aerodynamic characteristics. Measurements and calculations are conducted on the wide canard model for three canard horizontal positions: 1) apex of canard at the same horizontal position of the apex of wing, $X = 0$;

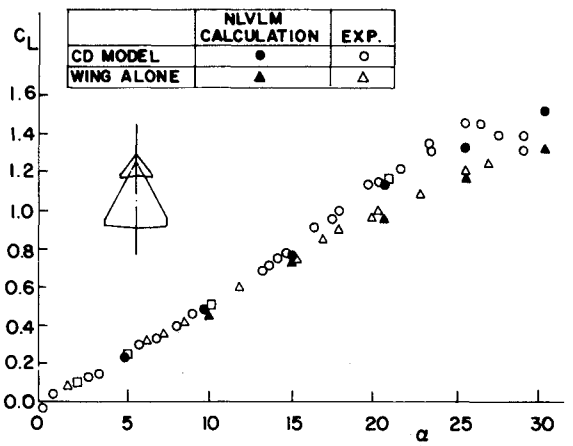

Fig. 4 Lift coefficient of the cropped delta model.

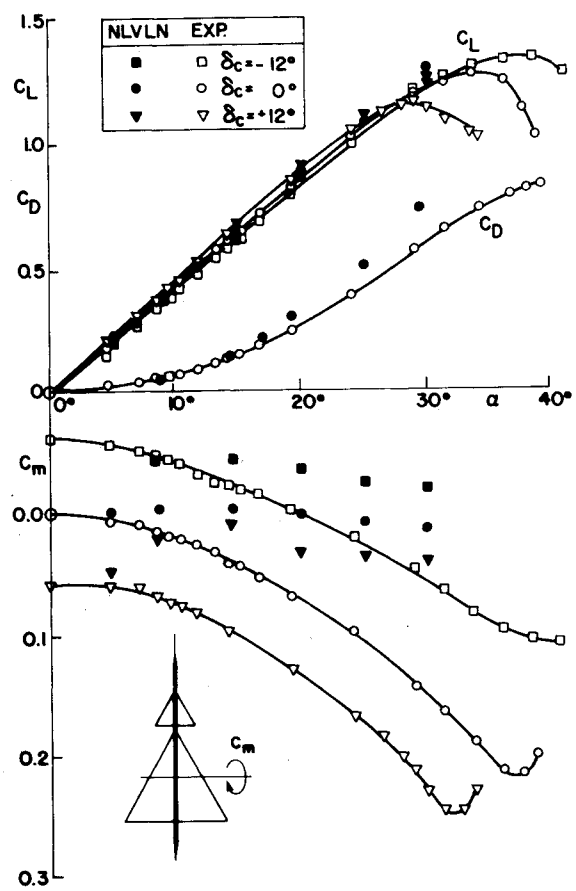

Fig. 5 Aerodynamic coefficients of the wing-canard European model A at various canard deflections.

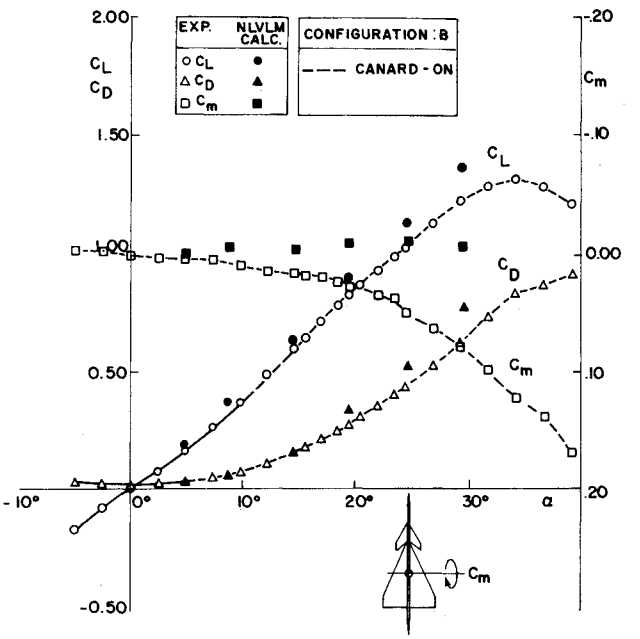

Fig. 6 Aerodynamic coefficients of the wing-canard European model B at zero canard deflection.

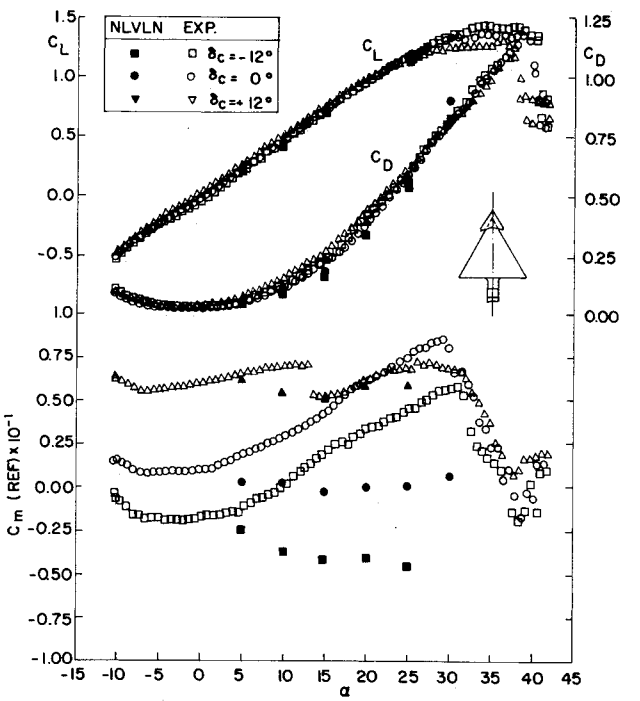

Fig. 7 Aerodynamic coefficients of the wide canard model for canard deflections of −10, 0, +15 deg and $X = -0.1$.

2) apex of canard 10% of wing root chord ahead of wing apex, $X = -0.1$; and 3) apex of canard 37% of wing root chord ahead of wing apex, $X = -0.37$. On the narrow canard model two horizontal positions of the canard apex, at 25 and 73% of wing root chord ahead of the wing apex, $X = -0.25$ and -0.73 are used. The results indicate that as the canard is moved forward, the lift and drag coefficients variation is not affected much, and only the maximum lift coefficient increases slightly. The increase in the maximum lift coefficient is about 10% at the most forward position for both the wide canard and narrow canard models. Therefore, only the comparisons of the measurements with the calculated results for the wide canard positioned at $X = -0.1$ are shown in Fig. 7, and for the narrow canard positioned at $X = -0.25$ in Fig. 8. The measurements show that the canard deflection has practically

no effect on the lift coefficients up to very close to the maximum lift, while the maximum lift coefficient is slightly higher for positive canard deflection. There is an increase in the induced drag particularly at higher angles of attack as the canards are deflected and there is a marked effect on the pitching moment—higher moments for positive deflection and lower moments for negative deflection. It is seen that the lift force on the wing-canard configuration remains almost independent of the relative angle between the canard and the wing because the lift forces on the canard increase as the canard angle of attack increases, while the lift on the wing decreases so as to cancel most of the additional lift of the canard. The NLVLM calculations results are in very good agreement for the lift and induced drag data, however, there is a large difference in the pitching moments. This large difference in the pitching moments can be also deduced from the large differences between the calculated and measured pressure distributions (presented in Fig. 9) for the wide canard configuration. The calculated pressure distribution fail to obtain the high suction on the forward part of the wing. On the rear part of the wing the calculations seem to spread the low pressure due to the vortex over a larger part of the span and shift the much lower peak inwards. The "spread" of the suction over the wing in the NLVLM calculation results in lift values which are found to be in reasonable agreement with the experimental data, but there is a large difference in the pitching moment. It should be noted that the differences between the measured and calculated positions of the aerodynamic center are in the range of 2–5% of the mean aerodynamic chord.

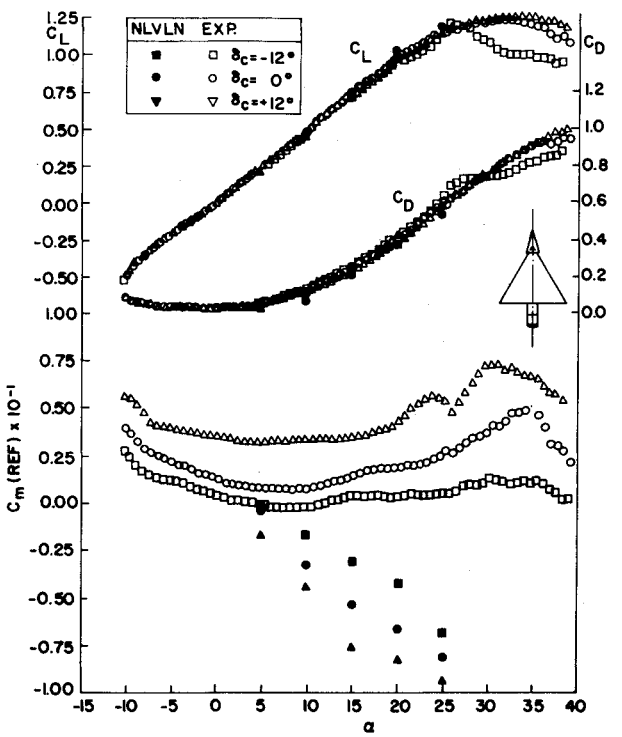

Fig. 8 Aerodynamic coefficients of the narrow canard model for canard deflections of −10, 0, +15 deg and $X = -0.25$.

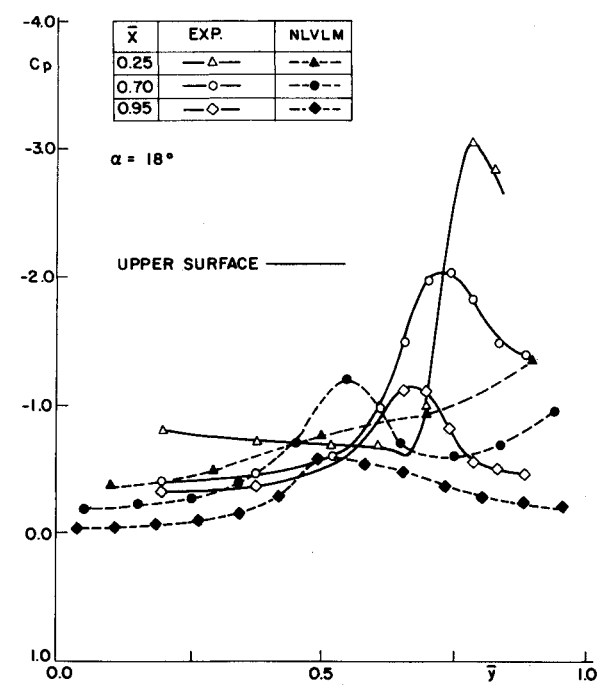

Fig. 9 Pressure distribution on the wing of the wide canard wing-canard model B at α = 18 deg.

Photographs of the positions of the cores of the canard and wing vortices above the wing surface using a schlieren optical system were presented in Ref. 17. Some indications as to the ability of the NLVLM to obtain the vortex trajectories can be seen from the side-by-side comparison of the measured vortex core positions with the calculated vortex trajectories on the narrow canard model as shown in Fig. 10. It can be seen that the calculated vortex trajectories emanating from the canard into its wake (describing the canard vortex) and flowing over the wing—shown in the right side, seem to agree reasonably well with the position of the core obtained in the schlieren photograph—shown in the left side. However, the rolling up of the vortex trajectories emanating from the leading edge of the wing is seen to be very slow on the forward part of the wing so that the rolling up is delayed to the rear part of the wing. This discrepancy in the vortex trajectories can be used to explain the discrepancies in the pressure dis-

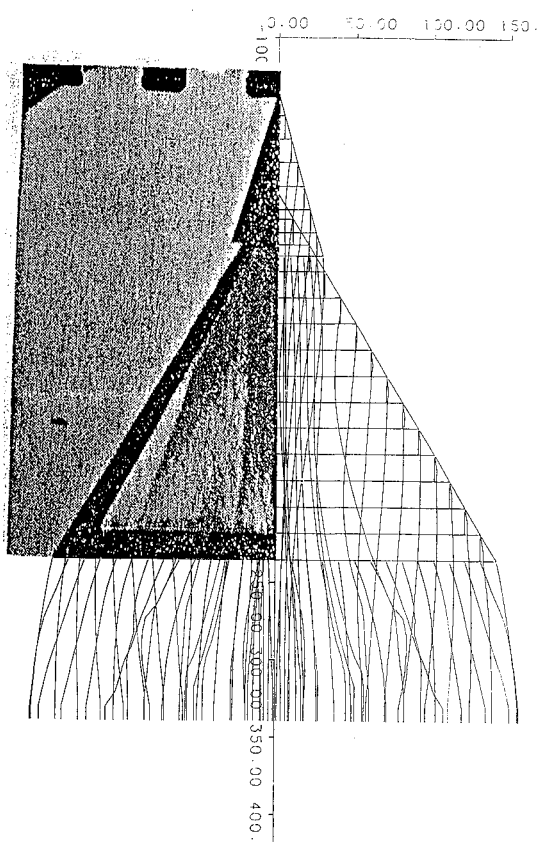

Fig. 10 Schlieren photograph visualization of vortex cores on the narrow canard model at α = 17 deg—left side; and the calculated vortex trajectories by the NLVLM—right side.

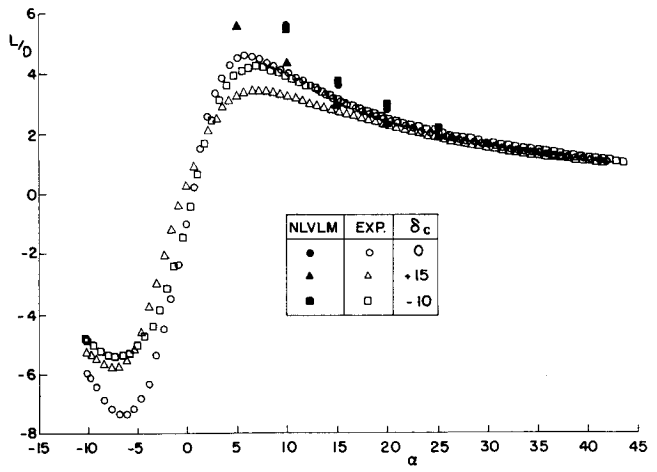

Fig. 11 *L/D* ratio variation with angle of attack for the wide canard model.

tributions and in the evaluation of the pitching moment, as discussed previously.

In addition to the maximum lift and the pitching moments which are affected by the canard and by its deflections, a most interesting effect is observed in the variation of the *L/D* ratio at various canard deflection angles as a function of the angle of attack as presented in Fig. 11 for the wide canard model. The experimental results show a relatively large reduction of the *L/D* ratio due to positive (and somewhat less for negative) canard deflection for an angle-of-attack variation between 2–10 deg with some effect maintained up to 15 deg.

Conclusions

The present study of various wing planforms and wing-canard configurations and the comparison between the aerodynamic characteristics evaluated by the NLVLM program and the experimental measurements can be used to examine the merit of the NLVLM as a working program for aerodynamic analysis. Although the fuselage was not included in the present study, it is possible to simulate a complete aircraft configuration by the NLVLM program.

The studies of the wing-canard configurations indicate that a positive canard deflection causes a slight increase in the maximum lift of the configuration while having only small effect on the variation of the lift as a function of angle of attack. There is also an increase in the induced drag particularly at high angles of attack. The main effect is the variation of the pitching moments due to canard deflection angles. There is also a very interesting effect of a marked decrease of the *L/D* ratio at positive canard deflections for small-to-moderate angles of attack.

The evaluation of the usefulness of the NLVLM program by the comparisons of the calculation results with the experimental data shows that the NLVLM program can be used to estimate the lift and induced drag of wing-canard configurations reasonably well. It is also shown that this method works even better on isolated wings in that the pitching moment can also be well-predicted.

Considering the fact that the NLVLM program requires much less computer resources and can be used with very short turnaround time in comparison with Euler code calculations, these lead to the conclusion that this analysis tool can potentially be of use in the design by analysis process employed during the preliminary design for wing-canard configurations.

References

[1]Rizzi, A., Eriksson, L. E., Schmidt, W., and Hitzel, S. M., "Simulating Vortex Flows Around Wings," AGARD CP 342, Nevilly Sur Seine, France, April 1983, pp. 21.1–21.14.

[2]Murman, E. M., and Rizzi, A., "Application of Euler Equations to Sharp Edge Delta Wings with Leading Edge Vortices," AGARD Symposium on Application of Computational Fluid Dynamics in Aeronautics, Aix-en-Provence, France, April 1986.

[3]Scherr, S., and Das, A., "Basic Analysis of the Flow Fields of Slender Delta Wings Using the Euler Equations," *Proceedings of the 16th ICAS Congress*, ICAS Paper 88-5.9.2, Jerusalem, Israel, Aug. 1988, pp. 1428–1436.

[4]Lee, K. D., and Brandt, S. A., "Modeling of Vortex Dominated Flow Fields in the Euler Formulation," *Proceedings of the 16th ICAS Congress*, ICAS Paper 88-5.9.3, Jerusalem, Israel, Aug. 1988, pp. 1437–1450.

[5]Kandil, O. A., and Chuang, A. H., "Influence of Numerical Dissipation on Computational Euler Equations for Vortex Dominated Flows," *AIAA Journal*, Vol. 25, No. 11, 1987, pp. 1426–1434.

[6]Gordon, R., and Rom, J., "Calculation of Aerodynamic Characteristics of Wings with Thickness and Camber by a New Method Based on the Modified Vortex Lattice Method," Technion—Israel Inst. of Technology Rept., Technion Aeronautical Engineering 493, Haifa, Israel, July 1982.

[7]Gordon, R., and Rom, J., "Calculation of Non-Linear Subsonic Characteristics of Wings with Thickness and Camber at High Incidence," *AIAA Journal*, Vol. 23, No. 6, 1985, pp. 817–825.

[8]Almosnino, D., and Rom, J., "Calculation of Symmetric Vortex Separation Affecting Subsonic Bodies at High Incidence," *AIAA Journal*, Vol. 21, No. 3, 1983, pp. 398–406.

[9]Almosnino, D., "High Angle of Attack Calculations of the Subsonic Flow on Slender Bodies," *AIAA Journal*, Vol. 23, No. 8, 1985, pp. 1150–1156.

[10]Melamed, B., "Investigation on the Convergence of Nonlinear Vortex Lattice Method," M.Sc. Thesis, Dept. of Aerospace Engineering, Technion—Israel Inst. of Technology, Haifa, Israel, 1991.

[11]Margason, R. J., and Lamar, J. E., "Vortex Lattice Fortran Program for Estimating Subsonic Aerodynamic Characteristics of Complex Planforms," NASA TN D-4739, Aug. 1968.

[12]Almosnino, D., and Rom, J., "Subsonic Aerodynamic Prediction of Shuttle-Like Configurations Using Non-Linear Vortex Lattice Method," *Proceedings of the 16th Congress of ICAS*, ICAS Paper 88-4.4.2, Jerusalem, Israel, Aug. 1988, pp. 638–643.

[13]Rom, J., and Gordon, R., "High Angle of Attack Non-Linear Vortex Lattice Calculations of Canard-Wing," AIAA Paper 88-0484, Reno, NV, Jan. 1988.

[14]Hummel, D., and Oelker, H. C., "Vortex Interference Effects on Close-Coupled Canard Configurations in Incompressible Flow," *Proceedings of the International Vortex Flow Experiments on Euler Code Validation*, Stockholm, Sweden, Oct. 1986, pp. 47–61.

[15]Oelker, H. C., and Hummel, D., "Investigation on the Vorticity Sheets of a Close-Coupled Delta Canard Configuration," *Proceedings of the 16th ICAS Congress*, ICAS Paper 88-5.4.1, Jerusalem, Israel, Aug. 1988, pp. 649–662.

[16]Drougge, G., "The International Vortex Flow Experiment for Computer Code Validation," ICAS Von-Karman Lecture, *Proceedings of the 16th ICAS Congress*, Paper 88-0.5, Jerusalem, Israel, Aug. 1988, pp. 35–41.

[17]Er-El, J., and Seginer, A., "The Leading Edge Vortex Trajectories and Breakdown Characteristics of Close-Coupled Wing-Canard Configurations," *Journal of Aircraft*, Vol. 22, No. 8, 1985, pp. 641–648.

[18]Rom, J., and Er-El, J., "Aerodynamic Characteristics of Close Coupled Canard Configurations Measured in the Subsonic Wind-Tunnel," Technion Aeronautical Engineering Rept. 637, Haifa, Israel, Dec. 1990.

[19]Rom, J., Er-El, J., and Gordon, R., "Measurements of the Aerodynamic Characteristics of Various Wing-Canard Configurations and Comparison with NLVLM Results," AIAA Paper 89-2217, Seattle, WA, Aug. 1989.

[20]Er-El, J., "Effect of Wing/Canard Interference on the Loading of a Delta Wing," *Journal of Aircraft*, Vol. 25, No. 1, 1988, pp. 18–24.